Manuscript prepared for The Cryosphere
with version 2014/09/16 7.15 Copernicus papers of the LaTeX class copernicus.cls.
Date: 27 June 2015

Using drones to map snow depth variability at cm resolution: an evaluation at peak accumulation

C. De Michele[1], F. Avanzi[1], D. Passoni[1], R. Barzaghi[1], L. Pinto[1], P. Dosso[2], A. Ghezzi[1], R. Gianatti[3], and G. Della Vedova[3]

[1]Politecnico di Milano, Department of Civil and Environmental Engineering, Piazza Leonardo da Vinci 32, 20133 Milano
[2]Studio di Ingegneria Terradat, Paderno Dugnano, Italy
[3]a2a Group, Grosio, Italy

Correspondence to: C. De Michele (carlo.demichele@polimi.it)

Abstract.

We investigate the snow depth distribution at the end of the accumulation season over a small alpine area ($\sim 3 \cdot 10^5$ m^2) using photogrammetry-based surveys at cm resolution with Unmanned Aerial Systems (U.A.S., also known as drones). Although these systems are growing in popularity as inexpensive alternatives to existing techniques within the field of remote sensing, the assessment of their performances in mapping snow depth distribution is still an open issue. We have designed two field campaigns during the 2013/2014 snow season. In the first survey, run before the beginning of the accumulation season, the digital elevation model of the ground has been obtained. The second survey, at peak accumulation, allowed to estimate the snow depth distribution as difference with respect to the previous aerial survey. We collected 12 manual measurements of snow depth at random positions to run a preliminary evaluation of U.A.S.-based snow depth estimations. In addition, we have explored how some basic snow depth statistics (e.g., mean, standard deviation, minima and maxima) change with sampling resolution (from 5 cm up to $\sim$100 m). The spatial integration of U.A.S. snow depth measurements allowed to estimate the snow volume accumulated over the area, that has been compared with the estimations by traditional interpolation of probes measurements. Results show that using U.A.S. seems to provide a fairly accurate estimation of point snow depth values (the average difference with reference to manual measurements is -7.3 cm). Moreover, we observe that, for our case study, snow depth standard deviation (hence coefficient of variation) increases with decreasing sampling distances, although it stabilizes for sampling distances smaller than 1 m. Interpolations of snow probe data return average differences in snow volume estimation, with respect to the one obtained through the U.A.S. system, equal to $\sim 21\%$.

1 Introduction

Seasonal snow accumulation and ablation dynamics are highly variable in space and time (Elder et al., 1991; Fassnacht et al., 2009; Grünewald et al., 2010; Mott et al., 2011; Grünewald et al., 2013; Scipión et al., 2013; Winstral et al., 2013). This variability plays a key role, among others, in avalanche prediction (Schweizer et al., 2008), in the routing of melt water in snowpacks (Katsushima et al., 2013; Avanzi et al., 2014a; Hirashima et al., 2014), in melt-runoff modeling (Lundquist and Dettinger, 2005), and in the evaluation of snow water equivalent distribution on complex terrains (Bavera et al., 2014).

The principal forcings ruling the spatial heterogeneity in the seasonal snowpack include 1) orographic effects (Lehning et al., 2008; Mott et al., 2014), 2) elevation, that rules the rain-snow transition zone, i.e. the elevation which separates snow- and rain-dominated areas during winter (Marks et al., 2013; Hinckley et al., 2014; Klos et al., 2014), 3) aspect and shadows from surrounding terrain (Hock, 1999; Marsh et al., 2012), which influence the exposure to radiation input from the Sun, hence varying melting rates, 4) wind redistribution (Lehning et al., 2008; Mott and Lehning, 2010), 5) avalanche transport (Lehning and Fierz, 2008; Grünewald et al., 2013) and 6) vegetation (Golding and Swanson, 1986; Ellis et al., 2010; Pomeroy et al., 2012).

The spatial distribution of snow depth and snowpack mass content, in the form of Snow Water Equivalent, SWE, has been widely measured and modeled, both at the local, slope and catchment scale (Grünewald et al., 2010). Modeling techniques include statistical approaches, such as Carroll and Cressie (1996); Elder et al. (1998); Erxleben et al. (2002); Anderton et al. (2004); Molotch et al. (2004); Dressler et al. (2006); López Moreno and Nogués-Bravo (2006); Skaugen (2007); Bavera et al. (2014), and conceptual, or physically-based models, e.g. Lehning et al. (2006, 2008). These works have improved our knowledge about, e.g., the relevance of single forcings in determining the distribution of the snow cover on complex terrains (Anderton et al., 2004). In addition, they provide a useful tool to estimate the impact of future modifications of climate on the Earth system (Bavay et al., 2009, 2013).

However, the run of a model usually needs input data to be available at a fine temporal resolution (say, daily or hourly). This can be obtained by means of automated devices, such as snow pillows (Cox et al., 1978; De Michele et al., 2013), cosmic ray counters (Morin et al., 2012) and ultrasonic depth sensors (Ryan et al., 2008). These devices are usually placed in areas that are believed to be suitable locations for representative measurements at wider scales (i.e., unaffected by local heterogeneities). Nonetheless, their spatial resolution is often sparse, while Grünewald and Lehning (2014) show that, usually, point stations on flat areas tend to overestimate catchment mean snow depth, and that representative cells are usually randomly located, i.e. impossible to be determined *a priori*. These represent important drawbacks of point weather stations in the study of snowpack dynamics (see Rice and Bales (2010); Meromy et al. (2013); Grünewald and Lehning (2014) and references therein). Moreover, such instruments are usually affected by systematic and random errors

(Cox et al., 1978; Fassnacht, 2004; Johnson, 2004), that decrease the actual precision of measurements with respect to instrumental resolution (Avanzi et al., 2014b).

Consequently, increasing interest is nowadays growing around distributed measurements of snow extent, depth and SWE (Dietz et al., 2012), able to substitute, or integrate, point, and usually sparse, measurements of these quantities. Tested techniques include terrestrial or airborne laser scanning (see e.g. Hopkinson et al. (2004); Deems et al. (2006); Prokop et al. (2008); Dadic et al. (2010); Grünewald et al. (2010); Lehning et al. (2011); Hopkinson et al. (2012); Deems et al. (2013); Grünewald et al. (2013); Grünewald and Lehning (2014); Hedrick et al. (2014)), SAR (Synthetic Aperture Radar, Luzi et al. (2009)), aerial photographies (Blöschl and Kirnbauer, 1992; König and Sturm, 1998; Worby et al., 2008), time-lapse photography (Farinotti et al., 2010), optical and micro-waves data from satellite platforms (Parajka and Blöschl, 2006; Dietz et al., 2012). Although these techniques (especially laser scanning) have widely demonstrated to be able to map snow depth variability, survey expenses and the expertise needed to operate them are still relevant issues that hamper their extensive use (Hood and Hayashi, 2010). As for satellite-based data, spatial resolution is a well-known limiting factor. In this perspective, automated, inexpensive and repeatable surveys at a fine spatial resolution (say, a centimetric resolution both in the horizontal and vertical direction) are still an open target of research, that could substantially improve our degree of knowledge of physical processes at the local scale by means of enhanced monitoring capabilities.

Unmanned Aerial Systems (U.A.S., also known as drones) could potentially fulfill all these requirements. These systems provide an inexpensive airborne support for sensors operating at different wavelengths, that can autonomously determine its own position in a 3D reference, reproduce a pre-arranged flight plan, and reconstruct a high-resolution Digital Surface Model (hereinafter, DSM) of a given area (Watts et al., 2012) by setting a suitable (low) flight height over the target (say, $\sim$100 m). All these features can potentially allow for automated, repeteable, cheap (Colomina and Molina, 2014) and low-risk surveys to be run, even in areas which are inaccessible for many other techniques. Their main novelty resides in the features of the support (especially, self-conduction and low cost), while the method used to retrieve points coordinates (e.g., photogrammetry) are usually rather traditional. Their use is nowadays rapidly increasing (Eisenbeiss, 2009; Watts et al., 2012; Colomina and Molina, 2014). Some examples regard ecology (Dunford et al., 2009; Koh and Wich, 2012), coastal engineering (Delacourt et al., 2009), geomorphological mapping (Lejot et al., 2007; Hugenholtz et al., 2013) or dust detection (Di Mauro et al., 2015). See Colomina and Molina (2014) for an exhaustive review. In optical surveys, they usually adopt compact digital cameras, due to the limited payload (say $\sim 10^2$ g). Nonetheless, these are affected by higher deformations as compared with those of photogrammetric calibrated cameras (Pollefeys et al., 1999; Remondino, 2006; Stretcha et al., 2010; Sona et al., 2014).

Here, we investigate the possibility of using drones to measure snow depth patterns at the end of the accumulation season within a small mountainous basin, using a centimetric resolution. This attempt addresses the following objectives: 1) to evaluate if these devices can be used to return a quantitative estimation of snow depth over a small area using photogrammetry, and 2) to investigate some basic statistical properties of snow distribution at varying spatial resolution (from 5 cm up to ∼100 m). 5 cm, as well as 10 or 20 cm (i.e., the resolutions we considered in this survey) are very fine with respect to other existing data-sets of snow depth (see López Moreno et al. (2015) as an example), and this can provide useful indications for future surveys using the same devices. In particular, we are interested in assessing whether a finer-than-usual spatial resolution provides an added value for hydrological applications. We chose as a field test the bare plateau around the Malghera lake, within the western Val Grosina valley (around 2300 m a.s.l.), northern Italy. A double airborne survey of this area, before and at the end of the accumulation season, was designed. During the first one, on 26th September 2013, the DSM of the ground has been collected, while during the second one, on 11th April 2014, the same area has been surveyed again to determine the DSM of the snow cover. Then, calculating the vertical differences between the two DSMs (Deems et al., 2013), the spatial distribution of snow depth has been derived, and compared with manual measurements at 12 points. These locations have been randomly chosen. Successively, the snow volume accumulated over the area was determined. Snow depth statistics (i.e., mean, standard deviation, coefficient of variation, minimum and maximum values) have been calculated at different (rescaled) spatial resolutions, and compared to evaluate how they vary across different orders of magnitude (i.e., from 5 cm to 100 m). Moreover, the snow volume estimated by the U.A.S. system has been compared to those provided by classical interpolation techniques (namely arithmetic mean, inverse distance weighting, Thiessen method and kriging) of point measurements. Interpolating spatially sparse measurements is one of the typical techniques used to estimate snow depth (or SWE) for operational applications, hence our interest for a comparison.

2 The study area

The case study is located in the western Val Grosina valley, Lombardy region, northern Italy. It is nearby the Malghera lake, $\sim 46°20'2''$ N, $\sim 10°7'14''$ E, 2320 m a.s.l. We chose this study area since it is at an elevation that guarantees an adequate snow thickness at the end of the accumulation season. Moreover, it is easily accessible during all the seasons. The approximate extent of the study area is $30 \cdot 10^4$ m^2. In Fig.1, the location of the study area is given, together with the topographic map of the ground, produced by the local regional administration (Lombardia region). Fig. 1 shows that site topography is relatively homogeneous.

3 Methods

3.1 Design of the surveys

The U.A.S. used in the two surveys is a light-weight fixed wing SwingletCAM system (SenseFly®). It is characterized by a limited weight (∼500 g) and size (wingspan equal to 80 cm). These features make it suitable to perform photogrammetric flights over limited areas (about 1 km^2) at a very high spatial resolutions (3-7 cm of Ground Sample Distance - GSD). The device is mainly made by an expanded polypropylene (EPP) foam, a carbon structure and composite parts. The propulsion is electric, with a maximum flight time around 30 minutes. The nominal cruise speed is ∼36 km/h, with a wind resistance up to 25 km/h and a radio link range up to 1 km from the master station on the ground. The SwingletCAM is able to perform pre-planned flights in a fully automated mode, since it continuously analyzes data from the onboard GPS/IMU system. However, the operator can always recover full control of the system. It incorporates a compact camera Canon Ixus 220HS (12 Mp and fixed focal length of 4.0 mm) which can acquire images at a GSD of some cm (depending on flight height). The camera uses a bandpass filter for the three colors RGB. These are placed ahead of the complementary metal–oxide–semiconductor (CMOS) according to a Bayer filter.

In these two field surveys, the GSD was set to 4.5 cm. This is because such a value allows to run a survey at a flying elevation of around 130 m above ground level (the complete range of the height values is between 130 m and 135 m), and this is a good safety condition for this U.A.S. device in a mountain area that is potentially subjected to strong winds. To gain the maximum stereoscopy and to avoid uncovered areas, forward and side overlaps were set to 80%. Following this approach, from six to seven strips were necessary to cover the area of interest.

3.2 DSMs production

For both the surveys, the flight lasted around 15–20 minutes. We report in Fig. 2 the location of camera photos and their overlap for each of the two surveys. In particular, the left panel regards the survey made on September 2013, while the right panel refers to the survey run during April 2014. Colors indicate the number of images covering each area. It is well known that the precision in coordinates estimation increases with an increasing number of images in which a point is present (Remondino and El – Hakim, 2006). In this perspective, most of the study area has been imaged at least by 3 or 4 images. Clearly, the overlap increases at the center of the study area. In that area, points have been imaged by a number of images ≥ 9.

In the survey made on September 26th 2013, the U.A.S. collected a block of 47 images divided in 6 strips. Due to the high image overlap, all the ground points are visible in many images (from 3 to 9). Thirteen pre-signalized Ground Control Points (henceforth, GCPs), measured through GPS rapid static survey, allowed the referencing of the block and the accuracy analyses. The standard deviation of the three coordinates of GCPs are around 3 cm in the horizontal components, and 5 cm in the vertical one.

In the survey run on April 11th 2014, the U.A.S. collected a block of 84 images divided in 12 strips (6 regular strips as in the autumn survey plus 6 cross strips). Fourteen pre-signalized GCPs, measured through a GPS static survey and theodolite, allowed the referencing of the block. This set of GCPs is different from the one used during the first survey. We chose points that were reasonably distributed over the area, and we referred them to the same reference frame. Based on this survey, GCPs coordinates have been estimated with a standard deviation of about 1 cm.

The blocks of images were processed using the Agisoft Photoscan software. This is a 3D modelling software that enables the exterior orientation of large datasets, by carrying out the image relative orientation, together with the self-calibration, in an arbitrary reference system, which is often obtained using a minimum constraint coming from the approximate orientation provided by the telemetry. Details about the processing procedure can be found in the Photoscan user manual (Agisoft, 2014), as well as at the Agisoft website (http://www.agisoft.com/). Moreover, a plenty of papers are available that describe the use of Photoscan to generate 3D models of surfaces (Verhoeven, 2011; Koutsoudis et al., 2014). Firstly, for each block of images, the position of the camera for each image is determined searching common points on the images. Then the extraction of topographic points (which represent a cloud of points), and the rejection of outliers are made for each survey. The subsequent use of GCPs allows translating and rotating the photogrammetric blocks in a specific reference frame, i.e. ETRF2000. Then, starting from the cloud of points, DSMs at different spatial resolutions (5, 10 and 20 cm) are extracted by generating a polygonal mesh model from the cloud data through interpolation. By making the differences of the two DSMs (at the same spatial resolution), maps of snow depth distribution can be obtained.

3.3 Point data collection

During the April survey, 12 point manual measurements of snow depth were operated using probes. The locations of these measurements have been randomly chosen, but were distributed as much as possible over the study area. Their spatial coordinates were obtained by total station theodolite observations referred to GPS baselines that were surveyed by static approach (40 minutes sessions). The accuracy of the obtained coordinates is of the order of 2-3 cm (i.e., comparable with the spatial resolution of the DSM at the maximum resolution).

We have used these data to run a preliminary evaluation of the performances of the device in retrieving point values of snow depth by comparing the manual and U.A.S.-based estimations of snow depth at the same location. In this way, it is possible to determine the mean and standard deviation of the differences between manual and U.A.S.-based estimations of snow depth.

Snow probes have been often used since the beginning of snow field surveys in order to determine snow depth amount at a point (Church, 1933; Elder et al., 2009; López Moreno et al., 2011, 2013). Although they represent the most direct way to measure this quantity, the long time needed to operate these surveys (Deems et al., 2013) have caused their partial replacement with automated devices. A comparison with probe measurements has been often used to assess the performances of alternative techniques to describe snow depth dynamics (Elder et al., 2009; Deems et al., 2013). As examples, Prokop et al. (2008) used 90 bamboo sticks to record snow depth changes and to compare these with measurements from laser scanning and tachimetry over a $\sim 200 \cdot 200$ m^2 area, Bavera and De Michele (2009) considered 170 point snow depth measurements to validate snow distribution estimations at a basin scale (area 325 km^2, snow cover interesting $2/3$ of the total surface), while Gutmann et al. (2012) and Nievinski and Larson (2014) used manual measurements from either 4 or 1 snow probes respectively to evaluate GPS-based estimations of snow depth. In the literature, it is known how to determine the number of points that would theoretically be needed to get an estimation of mean snow depth within a certain error range (see Chang et al. (2005); López Moreno et al. (2011) as examples). On the contrary, no specific rule or common practice exists to determine the minimum number of manual snow depth measurements, over a given area, needed to evaluate whether a given remote sensed technique returns satisfactory performances or not. Although this amount of points allows for a preliminary evaluation of the performances, more data could help to assess the performances of this technique in a more extensive way.

Several studies have demonstrated that snow depth is somehow spatially correlated at short distances (López Moreno et al., 2011), and that weather, climatic and topographic factors can drive snow depth variability at different spatial scales (see the Introduction or the papers by Grünewald et al. (2010); López Moreno et al. (2013); Mott et al. (2014); López Moreno et al. (2015) as examples). However, we opted for a random sampling technique to avoid any external information influencing artificially the evaluation of the performances. Here, we consider the worst case (i.e., no information available).

On the same day, a snow pit was excavated, and a snow density profile was measured through gravimetry (using a cylindrical sample holder, 15 cm long and with a 7.5 cm diameter). Measurements were taken at ~20 cm intervals along 210 cm of snow depth at that point. Density values spanned between 330 $\mathrm{kg/m^3}$ and 570 $\mathrm{kg/m^3}$ (mean value ~ 450 $\mathrm{kg/m^3}$).

3.4 Spatial sampling and the estimation of snow depth statistics and volume

To assess how spatial sampling affects the retrieval of snow depth at peak accumulation, we consider three different tests as follows.

As a first step, we estimated mean snow depth, minimum and maximum values, and total snow depth volume using the three snow depth maps we obtained directly from the survey cloud of points (i.e., maps at 5, 10 and 20 cm resolutions). The aim of this first experiment is to determine if it is possible to find a trade-off between increasing spatial resolution (i.e., considering smaller pixels) and the amount of significant information retrieved from the survey.

As a second step, we repeatedly resampled the snow depth map using an increasing cell size, starting from the map at 5 cm resolution. To do this, we recursively aggregated cells by progressively doubling cell size, and estimating snow depth for each new cell using the mean of the snow depth of the aggregated cells. Consequently, we produced estimated snow depth distribution at the following cell sizes: 5 cm (the original one), 10 cm, 20 cm, 40 cm, 80 cm, 160 cm, 320 cm, 640 cm, 1280 cm, 2560 cm, 5120 cm, 10240 cm. Missing values were disregarded. In this way, it was possible to calculate mean snow depth (μ), its standard deviation (σ), the coefficient of variation (CV) and minimum(maximum) value within each of these maps. The main purpose of this calculation is to assess how snow depth variability evolves with increasing/decreasing cell size.

As a third step, we compare the estimates of snow volume by some simple spatial interpolation techniques of the 12 snow probes data with that obtained using the U.A.S. system. Spatial interpolation techniques are methods used in the literature to produce continuous maps of attributes starting from some point values. These methods have been widely used in snow hydrology operational applications to produce maps of snow depth variability (López Moreno and Nogués-Bravo, 2006) starting from point values of the same variable. These techniques include, among others, 1) the *Inverse Distance Weighting* mehod (IDW), that calculates the attribute at a given location as a function of the distance between that point and the locations where known values are given (Erxleben et al., 2002; Fassnacht et al., 2003; López Moreno and Nogués-Bravo, 2006; Bavera et al., 2014), 2) *Thiessen* method, that associates the data at a given location to a certain subset of points close to it (Elder et al., 1991), 3) *Kriging*, which estimates the unknown values by previously estimating (or assigning) a certain law of variation of the variable in space (the so-called variogram, Carroll and Cressie (1996); Balk and Elder (2000); Erxleben et al. (2002); López Moreno and Nogués-Bravo (2006)), 4) *Cokriging*, that adds to the variogram additional predictors, such as elevation or aspect (López Moreno and Nogués-Bravo, 2006), 5) *Cokriging of the residuals* (Erxleben et al., 2002) 6) *Spline*, that estimates unknown values by using a function that minimizes surface curvature (López Moreno and Nogués-Bravo, 2006), and 7) *TIN*, i.e. Triangular Irregular Networks (Marsh et al., 2012). Moreover, global methods such as regression-tree models, multivariate statistical analysis or linear models have been also applied (Erxleben et al., 2002; Fassnacht et al., 2003; Anderton et al., 2004; Dressler et al., 2006; López Moreno and Nogués-Bravo, 2006; Bavera et al., 2014), sometimes combined with remote sensed images (such as in Harshburger et al. (2010)). The techniques we consider here are inverse distance weighting, Thiessen method, and ordinary Kriging. In addition, we will consider also the arithmetic mean of snow depth measured at probes. We chose these techniques since they are straightforward to be interpreted. Moreover, they also represent probably the most used techniques in spatialization problems. The application of more complex techniques (e.g., cokriging) is also hampered by the paucity of ground truth data collected.

4 Results and discussion

4.1 DSMs evaluation

We report in Figures 3 and 4 the orthophotos for the autumn and the spring survey, respectively. Figure 5, panels (a), and (b), describes the related DSMs, both characterized by a pixel size of 5 cm. Red lines depict contour lines (10 m interval).

The autumn DSM (Fig. 5, panel (a)) shows a good coherence with the topographic map, produced by the regional administration, and reported as background. For example, rivers and Malghera Lake outlet are correctly located. This consideration holds from the quantitative point of view too, since contour lines of the topographic map (in black) and those of DSM (in red) are in agreement. A more effective comparison is reported in Figure 6, where U.A.S.-based contours (in red) are directly superimposed to the contours of the topographic map. This comparison shows that the agreement increases with steeper terrains. This DSM has been also compared with the 20m $\times$ 20m DSM of the Lombardia Regional Authority, which is based on the digitalization of this 1:10000 map. The statistics of the differences are coherent with the accuracy of this DSM (i.e. with a standard deviation of 1.2 m).

As for the spring survey (Fig. 4 and Fig. 5, panel b), a comparison with the topographic map is not straightforward, because of snow depth coverage. Nevertheless, rivers and lake outlet seems to have been correcty positioned, since they correspond to clear depressions in the DSM. The snow depth surface on this area is interested by patchy coverage of sand dust transported by wind storms. This is visible as brown areas in the ortophoto (Fig. 4), and has been of great help in referencing the images of the spring survey, providing common points on photographs. Clearly, the associated DSM shows contour lines which are different from those obtained during the September survey. This is an effect of snow depth presence on the ground, that causes a slight reduction in topography irregularities, too.

4.2 Snow depth map and point evaluation

Figure 7 reports a map of snow depth distribution over the study area (at 5 cm resolution). Different colors indicate different values of snow thickness (see the legend scale reported in the figure). Black dots indicate the location of the 12 manual measurements.

Snow depth shows a remarkable micro-topographic variability over the considered area (i.e., at distances comparable with maps resolution), although this is rather limited in extension (around 300 000 m^2), and characterized by bare soil and/or scarce vegetation. Most of the central area is characterized by an alternation of low and high values of snow thicnkess, that would be completely missed by sampling at probe positions, only. Clusters of high values of snow depth correspond to the location of rivers, or depressions in micro-topography. On the contrary, low snow depths are observed on topographic local maxima. Legend scale shows that micro-topographic differences can be equal to $\sim 2 - 3$ m. This illustrates the relevant variation of accumulation dynamics of snow depth, and the scarce representativeness of point measurements (Grünewald and Lehning, 2014).

We report in Table 1 a comparison between manual (H_M) and U.A.S. based ($H_{U.A.S.}$) snow depth measurements. Manual measurements are associated with a standard resolution of $\pm$ 1 cm. The average difference between measurements is equal to -7.3 cm, with an associated standard deviation of 12.8 cm. This result shows that drones seem able to locally estimate the snow depth values with a precision of $\sim$ 10 cm (at least at probe positions). Part of the difference could be explained by slight differences (at centimetric scale) in the position of manual measurements and U.A.S. estimates, and instrumental resolutions. Nonetheless, this precision is comparable with the order of magnitude of the precision (instrumental resolution and noise effect) of many automated sensors currently installed for point measurements of the same variable (Avanzi et al., 2014b). The snow depth value at probe positions varies between 1.48 and 2.11 m. This represents a reduced variability with respect to the complete range of variation of U.A.S. snow depth values. On the one hand, the location of probes was randomly chosen, and snow depth spatial patterns are hardly predictable a priori (Grünewald and Lehning, 2014). On the other hand, additional investigations are necessary to assess U.A.S. performances in case of, e.g., shallow or patchy snow cover conditions (see Section 5.1).

It is worth comparing this precision to those reported in the literature for other remote-sensing techniques, by taking laser scanning as an example, given the abundance of papers on this topic, and the fact that this is nowadays one of the most used techniques within this field. Prokop et al. (2008) state that the standard deviation between manual probing and terrestial laser scanning is up to 10 cm (for maximum distances of 300 m), while Grünewald et al. (2010) report a standard deviation of less than 5 cm when comparing terrestrial laser scanning surveys with tachimetry (for distances up to 250 m), and a standard deviation of 6 cm when comparing terrestrial and airborne laser scanning at peak accumulation. Moreover, Grünewald and Lehning (2014) mention that the vertical error of airborne laser scanning surveys of snow is usually below 30 cm, but can be larger in steep terrains. It follows that the preliminary evaluation of standard deviation we provide here seems in agreement with the one obtained when using a laser scanner. However, note that the area that we used for this first experiment is very limited, and at peak accumulation (when snow depth spatial differences are usually leveled). Moreover, the number of points we took cannot assess U.A.S. performances exhaustively, so that additional tests are needed to provide a more reliable estimation of σ, as well as a more exhaustive comparison with existing techniques.

4.3 Snow depth statistics

4.3.1 Test 1: trade-off between spatial resolution and topography description

Table 2 proposes a comparison in terms of number of pixels considered, average/maximum/minimum snow depth and the volume of snow estimated according to the three DSMs at 5, 10 and 20 cm that have been directly obtained form the cloud of points. Clearly, an increase of the spatial resolution would increase the number of pixels. Nevertheless, this seems to marginally affect the estimations of average/maximum/minimum snow depth, as also the estimation of the total volume of snow. Basing on these results, a spatial resolution of 20 cm seems to be the trade-off between the number of pixels considered (i.e., computational time) and the description of the snow micro-topography for the considered area.

4.3.2 Test 2: the effect of spatial sampling on snow depth statistics

We report in Figure 8 some examples of the snow depth maps, one would obtain by rescaling the original map at 5 cm by progressively doubling the cell size. While the three maps considered in the previous section were directly obtained during the survey processing, the maps we considered here were rescaled from one of these (the one at 5 cm resolution). In particular, we report the maps with a 640 cm resolution (panel a), 2560 cm resolution (panel b) and 10240 cm resolution (panel c). These maps show that, as expected, the larger the cell size, the lower the degree of detail in the spatial description. The coarsest map ($\sim$ 100 m resolution) retains only a small fraction of original spatial variability (i.e., a lower-than-average snow depth in the proximity of the Malghera Lake, and a greater-than-average snow depth on slopes), but most of the spatial patterns in snow depth are lost.

In Figure 9, we quantify this loss. This map has been produced by calculating the differences between the rescaled map at 5120 cm resolution and the original map at 5 cm. This figure shows that considering a $\sim$50 m sampling distance can lead to strong under/over estimations of local snow depth (up to -1.9, or 2.1 m, respectively). We found similar differences when using 10240 m as spatial resolution. Areas having high snow depth differences are located nearby rivers and/or topographic irregularities. However, Fig. 9 shows that it is difficult to find locations within the $\sim$50 m resolution map with a satisfactory approximation.

In Figures 10 and 11, we report statistics in terms of mean (μ), maximum and minimum snow depth, standard deviation σ and CV as a function of maps resolution. These quantities have been calculated by making the pooling of all the data available for each map. Figure 10 tells that μ is almost constant across all the resolutions. This effect is probably due to the algorithm we used for the aggregation, that estimates the snow depth for an aggregated cell as the mean of the cells to be aggregated. Consequently, spatial differences are gradually homogenized when increasing the cell size. Minima and maxima are constant below 2 m and 10 m, respectively, but, for larger cell sizes, these quantities start to converge towards the mean.

However, Figure 11 shows that, within our case study, σ seems to present a well defined upper boundary (as well as CV). In particular, σ is minimum for coarser resolutions, and increases monotonously with smaller cell sizes. Nonetheless, it stabilizes when the cell size is $\leq$1 m. The CV has similar dynamics. In the literature, it has been observed that snow depth variability increases with higher sampling resolutions (López Moreno et al., 2015), but, to our knowledge, no data-set is still available with a sub-meter horizontal sampling resolution. Consequently, it is not possible for us to find confirmations of this behavior in previous analyses. However, if confirmed, it could help defining a lower boundary for sampling resolution to be considered when measuring snow depth during the accumulation season (say, 1 m resolution). This is an important direction of future investigations.

The range of CV that we found here is much lower than those reported by, e.g., López Moreno et al. (2015), but seems in agreement with the results by López Moreno et al. (2011) for a survey run during January. Snow depth spatial variability increases with time during the year (Ménard et al., 2014; López Moreno et al., 2015), due to local heterogeneity in ablation dynamics. It follows that a reduced CV during the winter season within a limited area can be expected.

4.3.3 Test 3: U.A.S.-based volume of snow vs. spatial interpolation

Table 3 reports the comparison between the estimated snow volume using a set of simple interpolation techniques of the 12 snow depth probes (namely, arithmetic mean, IDW, Thiessen method and ordinary Kriging) and the estimation of snow volume operated by the U.A.S. system (5 cm resolution). As we have already said, interpolating sparse measurements represent the typical method used in practical applications to determine the total volume of water in the snow form which could be potentially available for, e.g., hydropower production, irrigation or civil uses.

Results show that the differences among the estimates of different interpolation techniques are rather reduced. These are $\sim$ 1000 m^3, with the total volume equal to $\sim$ 360000 m^3. Nonetheless, all these techniques underestimate the snow volume estimated by the U.A.S. system ($\sim$ 460000 m^3). The average percentage difference in snow volume estimation, with respect to the one estimated by the U.A.S. system, is equal to $\sim 21\%$. In terms of absolute values, the average difference is $\sim$ 96350 m^3. Considering an average bulk snow density of 450 kg/m^3 (as measured in the snow pit), this would entail an absolute difference in SWE estimation of $\sim$ 43358 m^3.

It is worth recalling that the considered area has a very reduced extension with respect to the usual distance between gauged sites in instrumental networks (see e.g. Fassnacht et al. (2003)). This result shows that the assessment of snow depth micro-topography has clear hydrological impacts on many applications of scientific as well as engineering interest and cannot be easily neglected. From this perspective, U.A.S. systems confirm to be able to easily, cheaply, and semi-automatically return a more refined representation of snow depth.

Table 3 shows that all interpolation techniques return an underestimated volume of snow. This is a case-specific result, that is due to the choice of probe positions. In fact, Figure 7 shows that manual measurements were taken in areas that were mainly characterized by shallow snow cover. Since evaluating *a-priori* representative locations is very difficult (Grünewald and Lehning, 2014), and since they could even vary from year to year basing on snow redistribution dynamics, this result shows again the advantage of using a directly distributed estimation instead of relying on a simplified representation of snow topography.

5 Conclusions

For the first time, we have here mapped snow depth variability at cm scale by means of a photogrammetry-based survey using drones. For this purpose, we run two surveys. The first one, during September 2013, allowed to reconstruct the topography of the ground. This survey will not be necessary for future assessment of snow distribution in the same area. Then, during April 2014, a second survey allowed to reconstruct the variability of snow depth, by vertical differentiation of the maps.

Results show that: 1) ortophoto and DSM of autumn survey are in agreement with the topographic map available for the study area; 2) the average difference between manual and U.A.S. based measurements of snow depth (and the associated standard deviation) seems competitive with the typical precision of point measurements and other distributed techniques (the average difference obtained is equal to -7.3 cm, with an associated standard deviation of 12.8 cm); 3) the standard deviation (and CV) across the study area increases with decreasing spatial sampling distances, but stabilizes below 1 m resolution, thus suggesting the existence of a trade-off between increasing spatial resolution of surveys and the amount of significant information obtained for hydrological applications; 4) the evaluation of snow depth volume (hence, SWE) using classical interpolation techniques of randomly chosen point values of snow depth is severely biased due to the biases in point snow depth values chosen for the interpolation (average difference in snow volume estimation, with respect to the one estimated by the U.A.S., equal to ~ 21 %).

5.1 Outlook

The U.A.S. technology has some interesting potentialities within the framework of available methods to reconstruct the spatial variability of snow surface. In fact, this device allows to obtain semi-automated, quick and repeatable surveys of limited areas, with a quite high vertical precision. Although the device that we used here needs the operator to assist it during take-off operations, other devices (currently not available to the authors) can take off and land in an automated way, and can cover much wider areas. This could let repeated (say, daily) surveys to be autonomously obtained, even without needing an operator to reach the target area. This, together with the possibility to substitute, or integrate, optical sensors with sensors at different wavelengths, could represent in the future an alternative to automated point stations to directly obtain distributed measurements of snow variables. Moreover, attempts have been already made to design supports that could be able to resist to harsh climatic conditions (Funaki et al., 2008), such as strong winds, that would make unfeasible a survey using the same sensor used here.

Future developments should compare the performances of this technique with those obtained by other remote sensing approaches. The main reason is that this test has been run during just one day, and one location, in order to provide a preliminary assessment of the feasibility of using drones to retrieve snow depth over a limited area. No specific limitation seems to hamper the use of these devices over larger areas, apart from batteries duration, or within areas characterized by patchy snow cover conditions. Moreover, the fact that U.A.S. systems are basically a novel support to run traditional surveys (such as photogrammetry) improves our confidence towards these systems, their expected outcomes and precision.

However, different weather conditions (such as precipitation events, or scarce visibility), different snow cover conditions (such as shallow snow covers) and/or different topographic patterns could have an impact on the performances of these devices that must be still assessed. As an example, a shallow snow cover (say, snow depth lower than 20/30 cm) is likely to be difficult to be measured correctly given the standard deviation we found here (12.8 cm), while the presence of vegetation can create ambiguity in the mapping of snow. This could be solved by using optical data to detect snow covered areas, only. Moreover, scarce visibility can potentially undermine a photogrammetry-based survey given the difficulties in detecting the ground (or snow) surface from an elevation of around 100 m during, e.g., fog events or intense rainfalls (or snowfalls).

Acknowledgements. The Authors want to thank A2A for the logistic support during the set up of the experiment. We would like to thank Mr. Riccardo Capetti and Mr. Amilcare Marchetti (A2A) for their assistance during field activities. We would like to thank the Editor, Prof. Philip Marsh, Prof. Steven R. Fassnacht (referee) and an anonymous referee for their feedbacks on the manuscript.

References

Agisoft: Agisoft PhotoScan User Manual Professional Edition, Version 1.1, 2014.

Anderton, S. P., White, S. M., and Alvera, B.: Evaluation of spatial variability in snow water equivalent for a high mountain catchment, Hydrological Processes, 18, 435 – 453, doi:10.1002/hyp.1319, 2004.

Avanzi, F., Caruso, M., Jommi, C., De Michele, C., and Ghezzi, A.: Continuous-time monitoring of liquid water content in snowpacks using capacitance probes: A preliminary feasibility study, Advances in Water Resources, 68, 32–41, doi:10.1016/j.advwatres.2014.02.012, 2014a.

Avanzi, F., De Michele, C., Ghezzi, A., Jommi, C., and Pepe, M.: A processing modeling routine to use SNOTEL hourly data in snowpack dynamic models, Advances in Water Resources, 73, 16–29, 2014b.

Balk, B. and Elder, K.: Combining binary decision tree and geostatistical methods to estimate snow distribution in a mountain watershed, Water Resources Research, 36, 13 – 26, doi:10.1029/1999WR900251, 2000.

Bavay, M., Lehning, M., Jonas, T., and Löwe, H.: Simulations of future snow cover and discharge in Alpine headwater catchments, Hydrological Processes, 23, 95–108, doi:10.1002/hyp.7195, 2009.

Bavay, M., Grünewald, T., and Lehning, M.: Response of snow cover and runoff to climate change in high Alpine catchments of Eastern Switzerland, Advances in Water Resources, 55, 4 – 16, doi:10.1016/j.advwatres.2012.12.009, 2013.

Bavera, D. and De Michele, C.: Snow water equivalent estimation in the Mallero basin using snow gauge data and MODIS images and fieldwork validation, Hydrological Processes, 23, 1961–1972, doi:10.1002/hyp.7328, 2009.

Bavera, D., Bavay, M., Jonas, T., Lehning, M., and De Michele, C.: A comparison between two statistical and a physically-based model in snow water equivalent mapping, Advances in Water Resources, 63, 167–178, doi:10.1016/j.advwatres.2013.11.011, 2014.

Blöschl, G. and Kirnbauer, R.: An Analysis of snow cover patterns in a small alpine catchment, Hydrological Processes, 6, 99 – 109, doi:10.1002/hyp.3360060109, 1992.

Carroll, S. S. and Cressie, N.: Spatial modeling of snow water equivalent using covariances estimated from spatial and geomorphic attributes, Journal of Hydrology, 190, 42 – 59, doi:10.1016/S0022-1694(96)03062-4, 1996.

Chang, A. T. C., Kelly, R. E. J., Josberger, E. G., Armstrong, R. L., Foster, J. L., and Mognard, N. M.: Analysis of ground-measured and passive-microwave-derived snow depth variations in midwinter across the Northern Great Plains, Journal of Hydrometeorology, 6, 20–33, 2005.

Church, J. E.: Snow Surveying: Its Principles and Possibilities, Geographical Review, 23, 529 – 563, 1933.

Colomina, I. and Molina, P.: Unmanned Aerial Systems for Photogrammetry and Remote Sensing: a review, ISPRS Journal of Photogrammetry and Remote Sensing, 92, 79–97, doi:10.1016/j.isprsjprs.2014.02.013, 2014.

Cox, L., Bartee, L., Crook, A., Farnes, P., and Smith, J.: The care and feeding of snow pillows, in: Proceedings of the 46th Annual Western Snow Conference, pp. 40–47, Otter Rock, Oregon, 1978.

Dadic, R., Mott, R., Lehning, M., and Burlando, P.: Wind influence of snow depth distribution and accumulation over glaciers, Journal of Geophysical Research, 115, F01 012, doi:10.1029/2009JF001261, 2010.

De Michele, C., Avanzi, F., Ghezzi, A., and Jommi, C.: Investigating the dynamics of bulk snow density in dry and wet conditions using a one-dimensional model, The Cryosphere, 7, 433–444, doi:10.5194/tc-7-433-2013, 2013.

Deems, J. S., Fassnacht, S. R., and Elder, K. J.: Fractal Distribution of Snow Depth from Lidar Data, Journal of Hydrometeorology, 7, 285 – 297, doi:http://dx.doi.org/10.1175/JHM487.1, 2006.

Deems, J. S., Painter, T. H., and Finnegan, D. C.: Lidar measurement of snow depth: a review, Journal of Glaciology, 59, 467 – 479, doi:10.3189/2013JoG12J154, 2013.

Delacourt, C., Allemand, P., Jaud, M., Grandjean, P., Deschamps, A., Ammann, J., Cuq, V., and Suanez, S.: DRELIO: An Unmanned Helicopter for Imaging Coastal Areas, Journal of Coastal Research, Special Issue, 56, 1489–1493, 2009.

Di Mauro, B., Fava, F., Ferrero, L., Garzonio, R., Baccolo, G., Delmonte, B., and Colombo, R.: Mineral dust impact on snow radiative properties in the European Alps combining ground, UAV and satellite observations, Journal of Geophysical Research Atmospheres, doi:10.1002/2015JD023287, 2015.

Dietz, A. J., Kuenzer, C., Gessner, U., and Dech, S.: Remote sensing of snow - a review of available methods, International Journal of Remote Sensing, 33, 4094 – 4134, doi:10.1080/01431161.2011.640964, 2012.

Dressler, K. A., Leavesley, G. H., Bales, R. C., and Fassnacht, S. R.: Evaluation of gridded snow water equivalent and satellite snow cover products for mountain basins in a hydrologic model, Hydrological Processes, 20, 673 – 688, doi:10.1002/hyp.6130, 2006.

Dunford, R., Michel, K., Gagnage, M., Piegay, H., and Tremelo, M. L.: Potential and constraints of Unmanned Aerial Vehicle technology for the characterization of Mediterranean riparian forest, International Journal of Remote Sensing, 30, 4915–4935, 2009.

Eisenbeiss, H.: UAV Photogrammetry, 194, Institute of Geodesy and Photogrammetry, ETH Zürich, 2009.

Elder, K., Dozier, J., and Michaelsen, J.: Snow accumulation and distribution in an alpine watershed, Water Resources Research, 27, 1541–1552, doi:10.1029/91WR00506, 1991.

Elder, K., Rosenthal, W., and Davis, R. E.: Estimating the spatial distribution of snow water equivalence in a montane watershed, Hydrological Processes, 12, 1793–1808, 1998.

Elder, K., Cline, D., Liston, G. E., and Armstrong, R.: NASA Cold Land Processes Experiment (CLPX 2002/03): Field Measurements of Snowpack Properties and Soil Moisture, Journal of Hydrometeorology, 10, 320–329, 2009.

Ellis, C. R., Pomeroy, J. W., Brown, T., and MacDonald, J.: Simulation of snow accumulation and melt in needleleaf forest environments, Hydrology and Earth System Sciences, 14, 925 – 940, doi:10.5194/hess-14-925-2010, 2010.

Erxleben, J., Elder, K., and Davis, R.: Comparison of spatial interpolation methods for estimating snow distribution in the Colorado Rocky Mountains, Hydrological Processes, 16, 3627 – 3649, doi:10.1002/hyp.1239, 2002.

Farinotti, D., Magnusson, J., Huss, M., and Bauder, A.: Snow accumulation distribution inferred from time-lapse photography and simple modelling, Hydrological Processes, 24, 2087 – 2097, doi:10.1002/hyp.7629, 2010.

Fassnacht, S. R.: Estimating Alter-shielded gauge snowfall undercatch, snowpack sublimation, and blowing snow transport at six sites in the coterminous USA, Hydrological Processes, 18, 3481–3492, 2004.

Fassnacht, S. R., Dressler, K. A., and Bales, R. C.: Snow water equivalent interpolation for the Colorado River Basin from snow telemetry (SNOTEL) data, Water Resources Research, 39 (8), 1208, 2003.

Fassnacht, S. R., WIliams, M. W., and Corrao, M. V.: Changes in the surface roughness of snow from millimetre to metre scales, Ecological Complexity, 6, 221–229, 2009.

Funaki, M., Hirasawa, N., and the Ant Plane Group: Outline of a small unmanned aerial vehicle (Ant-Plane) designed for Antarctic research, Polar Science, 2, 129–142, 2008.

Golding, D. L. and Swanson, R. H.: Snow distribution patterns in clearings and adjacent forest, Water Resources Research, 22, 1931 – 1940, doi:10.1029/WR022i013p01931, 1986.

Grünewald, T. and Lehning, M.: Are flat-field snow depth measurements representative? A comparison of selected index sites with areal snow depth measurements at the small catchment scale, Hydrological Processes, n/a–n/a, n/a–n/a, doi:10.1002/hyp.10295, http://dx.doi.org/10.1002/hyp.10295, 2014.

Grünewald, T., Schirmer, M., Mott, R., and Lehning, M.: Spatial and temporal variability of snow depth and ablation rates in a small mountain catchment, The Cryosphere, 4, 215–225, doi:10.5194/tc-4-215-2010, 2010.

Grünewald, T., Stötter, J., Pomeroy, J. W., Dadic, R., Baños, I. M., Marturiá, J., Spross, M., Hopkinson, C., Burlando, P., and Lehning, M.: Statistical modelling of the snow depth distribution in open alpine terrain, Hydrology and Earth System Sciences, 17, 3005–3021, doi:10.5194/hess-17-3005-2013, 2013.

Gutmann, E. D., Larson, K. M., Williams, M. W., Nievinski, F. G., and Zavorotny, V.: Snow measurement by GPS interferometric reflectometry: an evaluation at Niwot Ridge, Colorado, Hydrological Processes, 26, 2951 – 2961, 2012.

Harshburger, B. J., Humes, K. S., Walden, V. P., Blandford, T. R., Moore, B. C., and Dezzani, R. J.: Spatial interpolation of snow water equivalency using surface observations and remotely sensed images of snow-covered area, Hydrological Processes, 24, 1285–1295, doi:10.1002/hyp.7590, 2010.

Hedrick, A., Marshall, H.-P., Winstral, A., Elder, K., Yueh, S., and Cline, D.: Independent evaluation of the SNODAS snow depth product using regional scale LiDAR-derived measurements, The Cryosphere Discussions, 8, 3141–3170, doi:10.5194/tcd-8-3141-2014, http://www.the-cryosphere-discuss.net/8/3141/2014/, 2014.

Hinckley, E.-L. S., Ebel, B. A., Barnes, R. T., Anderson, R. S., Williams, M. W., and Anderson, S. P.: Aspect control of water movement on hillslopes near the rain - snow transition of the Colorado Front Range, Hydrological Processes, 28, 74 – 85, doi:10.1002/hyp.9549, 2014.

Hirashima, H., Yamaguchi, S., and Katsushima, T.: A multi-dimensional water transport model to reproduce preferential flow in the snowpack, Cold Regions Science and Technology, 108, 80–90, 2014.

Hock, R.: A distributed temperature-index ice- and snowmelt model including potential direct solar radiation, Journal of Glaciology, 45, 101–111, 1999.

Hood, J. L. and Hayashi, M.: Assessing the application of a laser rangefinder for determining snow depth in inaccessible alpine terrain, Hydrology and Earth System Sciences, 14, 901–910, 2010.

Hopkinson, C., Sitar, M., Chasmer, L., and Treitz, P.: Mapping snowpack depth beneath forest canopies using airborne lidar, Photogrammetric Engineering and Remote Sensing, 70, 323 – 330, 2004.

Hopkinson, C., Collins, T., Anderson, A., Pomeroy, J., and Spooner, I.: Spatial Snow Depth Assessment Using LiDAR Transect Samples and Public GIS Data Layers in the Elbow River Watershed, Alberta, Canadian Water Resources Journal / Revue canadienne des ressources hydriques, 37, 69 – 87, doi:10.4296/cwrj3702893, 2012.

Hugenholtz, C. H., Whitehead, K., Brown, O. W., Barchyn, T. E., Moorman, B. J., LeClair, A., Riddell, K., and Hamilton, T.: Geomorphological mapping with a small unmanned aircraft system (sUAS): Feature detection and accuracy assessment of a photogrammetrically-derived digital terrain model, Geomorphology, 194, 16–24, doi:10.1016/j.geomorph.2013.03.023, 2013.

Johnson, J. B.: A theory of pressure sensor performance in snow, Hydrological Processes, 18, 53–64, doi:10.1002/hyp.1310, 2004.

Katsushima, T., Yamaguchi, S., Kumakura, T., and Sato, A.: Experimental analysis of preferential flow in dry snowpack, Cold Regions Science and Technology, 85, 206–216, doi:10.1016/j.coldregions.2012.09.012, 2013.

Klos, P. Z., Link, T. E., and Abatzoglou, J. T.: Extent of the rain-snow transition zone in the western U.S. under historic and projected climate, Geophysical Research Letters, Accepted manuscript, n/a–n/a, doi:10.1002/2014GL060500, http://dx.doi.org/10.1002/2014GL060500, 2014.

Koh, L. P. and Wich, S. A.: Dawn of drone ecology: low-cost autonomous aerial vehicles for conservation, Tropical Conservation Science, 5, 121–132, 2012.

König, M. and Sturm, M.: Mapping snow distribution in the Alaskan Arctic using aerial photography and topographic relationships, Water Resources Research, 34, 3471 – 3483, doi:10.1029/98WR02514, 1998.

Koutsoudis, A., Vidmar, B., Ioannakis, G., Arnaoutoglou, F., Pavlidis, G., and Chazmas, C.: Multi-image 3D reconstruction data evaluation, Journal of Cultural Heritage, 15, 73–79, 2014.

Lehning, M. and Fierz, C.: Assessment of snow transport in avalanche terrain, Cold Regions Science and Technology, 51, 240 – 252, doi:10.1016/j.coldregions.2007.05.012, 2008.

Lehning, M., Völksch, I., Gustafsson, D., Nguyen, T. A., Stähli, M., and Zappa, M.: ALPINE3D: a detailed model of mountain surface processes and its application to snow hydrology, Hydrological Processes, 20, 2111–2128, doi:10.1002/hyp.6204, 2006.

Lehning, M., Löwe, H., Ryser, M., and Raderschall, N.: Inhomogeneous precipitation distribution and snow transport in steep terrain, Water Resources Research, 44, W07 404, doi:10.1029/2007WR006545, 2008.

Lehning, M., Grünewald, T., and Schirmer, M.: Mountain snow distribution governed by an altitudinal gradient and terrain roughness, Geophysical Research Letters, 38, n/a–n/a, doi:10.1029/2011GL048927, http://dx.doi.org/10.1029/2011GL048927, 2011.

Lejot, J., Delacourt, C., Piégay, H., Fournier, T., Trémélo, M. L., and Allemand, P.: Very high spatial resolution imagery for channel bathymetry and topography from an unmanned mapping controlled platform, Earth Surface Processes and Landforms, 32, 1705–1725, 2007.

López Moreno, J. I. and Nogués-Bravo, D.: Interpolating local snow depth data: an evaluation of methods, Hydrological Processes, 20, 2217 – 2232, doi:10.1002/hyp.6199, http://dx.doi.org/10.1002/hyp.6199, 2006.

López Moreno, J. I., Fassnacht, S. R., Beguería, S., and Latron, J. B. P.: Variability of snow depth at the plot scale: implications for mean depth estimation and sampling strategies, The Cryosphere, 5, 617–629, 2011.

López Moreno, J. I., Fassnacht, S. R., Heath, J. T., Musselman, K. N., Revuelto, J., Latron, J., Móran-Tejeda, E., and Jonas, T.: Small scale spatial variability of snow density and depth over complex alpine terrain: Implications for estimating snow water equivalent, Advances in Water Resources, 55, 40–52, 2013.

López Moreno, J. I., Revuelto, J., Fassnacht, S. R., Azorín-Molina, C., Vicente-Serrano, S. M., Morán-Tejeda, E., and Sexstone, G. A.: Snowpack variability across various spatio-temporal resolutions, Hydrological Processes, 29, 1213–1224, 2015.

Lundquist, J. D. and Dettinger, M. D.: How snowpack heterogeneity affects diurnal streamflow timing, Water Resources Research, 41, W05 007, doi:10.1029/2004WR003649, 2005.

Luzi, G., Noferini, L., Mecatti, D., Macaluso, G., Pieraccini, M., Atzeni, C., Schaffhauser, A., Fromm, R., and Nagler, T.: Using a Ground-Based SAR Interferometer and a Terrestrial Laser Scanner to Monitor a Snow-Covered Slope: Results From an Experimental Data Collection in Tyrol (Austria), IEEE Transactions on Geoscience and Remote Sensing, 47, 382 – 393, doi:10.1109/TGRS.2008.2009994, 2009.

Marks, D., Winstral, A., Reba, M., Pomeroy, J., and Kumar, M.: An evaluation of methods for determining during-storm precipitation phase and the rain/snow transition elevation at the surface in a mountain basin, Advances in Water Resources, 55, 98 – 110, doi:http://dx.doi.org/10.1016/j.advwatres.2012.11.012, snow–Atmosphere Interactions and Hydrological Consequences, 2013.

Marsh, C. B., Pomeroy, J. W., and Spiteri, R. J.: Implications of mountain shading on calculating energy for snowmelt using unstructured triangular meshes, Hydrological Processes, 26, 1767 – 1778, doi:10.1002/hyp.9329, 2012.

Ménard, C. B., Essery, R., and Pomeroy, J.: Modelled sensitivity of the snow regime to topography, shrub fraction and shrub height, Hydrology and Earth System Sciences, 18, 2375 – 2392, doi:10.5194/hess-18-2375-2014, 2014.

Meromy, L., Molotch, N. P., Link, T. E., Fassnacht, S. R., and Rice, R.: Subgrid variability of snow water equivalent at operational snow stations in the western USA, Hydrological Processes, 27, 2383–2400, 2013.

Molotch, N. P., Fassnacht, S. R., Bales, R. C., and Helfrich, S. R.: Estimating the distribution of snow water equivalent and snow extent beneath cloud cover in the Salt - Verde River basin, Arizona, Hydrological Processes, 18, 1595 – 1611, doi:10.1002/hyp.1408, 2004.

Morin, S., Lejeune, Y., Lesaffre, B., Panel, J.-M., Poncet, D., David, P., and Sudul, M.: An 18-yr long (1993–2011) snow and meteorological dataset from a mid-altitude mountain site (Col de Porte, France, 1325 m alt.) for driving and evaluating snowpack models, Earth System Science Data, 4, 13–21, doi:10.5194/essd-4-13-2012, http://www.earth-syst-sci-data.net/4/13/2012/, 2012.

Mott, R. and Lehning, M.: Meteorological Modeling of Very High-Resolution Wind Fields and Snow Deposition for Mountains, Journal of Hydrometeorology, 11, 934 – 949, http://dx.doi.org/10.1175/2010JHM1216.1, 2010.

Mott, R., Egli, L., Grünewald, T., Dawes, N., Manes, C., Bavay, M., and Lehning, M.: Micrometeorological processes driving snow ablation in an Alpine catchement, The Cryosphere, 5, 1083–1098, doi:10.5194/tc-5-1083-2011, 2011.

Mott, R., Scipión, D., Schneebeli, M., Dawes, N., and Lehning, M.: Orographic effects on snow deposition patterns in mountainous terrain, Journal of Geophysical Research, 119, 1419–1439, doi:10.1002/2013JD019880, 2014.

Nievinski, F. G. and Larson, K. M.: Inverse Modeling of GPS Multipath for Snow Depth Estimation - Part II: Application and Validation, IEEE Transactions on Geoscience and Remote Sensing, 52, 6555 – 6563, 2014.

Parajka, J. and Blöschl, G.: Validation of MODIS snow cover images over Austria, Hydrology and Earth System Sciences, 10, 679–689, doi:10.5194/hess-10-679-2006, http://www.hydrol-earth-syst-sci.net/10/679/2006/, 2006.

Pollefeys, M., Koch, R., and Van Gool, L.: Self-calibration and metric reconstruction in spite of varying and unknown internal camera parameters, in: IJCV, Sixth International Conference on Computer Vision, pp. 90–95, Bombay, India, doi:10.1109/ICCV.1998.710705, 1999.

Pomeroy, J., Fang, X., and Ellis, C.: Sensitivity of snowmelt hydrology in Marmot Creek, Alberta, to forest cover disturbance, Hydrological Processes, 26, 1891 – 1904, doi:10.1002/hyp.9248, 2012.

Prokop, A., Schirmer., M., Rub, M., Lehning, M., and Stocker, M.: A comparison of measurement methods: terrestrial laser scanning, tachymetry and snow probing for the determination of the spatial snow-depth distribution on slopes, Annals of Glaciology, 49, 210 – 216, doi:10.3189/172756408787814726, 2008.

Remondino, F.: Detectors and descriptors for photogrammetric applications, ISPRS Archives, 36, 49–54, 2006.

Remondino, F. and El – Hakim, S.: Image-based 3D modelling: a review, The photogrametric record, 21, 269 – 291, 2006.

Rice, R. and Bales, R. C.: Embedded-sensor network design for snow cover measurements around snow pillow and snow course sites in the Sierra Nevada of California, Water Resources Research, 46, W03 537, 2010.

Ryan, W. A., Doesken, N. J., and Fassnacht, S. R.: Evaluation of Ultrasonic Snow Depth Sensors for U.S. Snow Measurements, Journal of Atmospheric and Oceanic Technology, 25, 667–684, doi:10.1175/2007JTECHA947.1, 2008.

Schweizer, J., Kronholm, K., Bruce Jamieson, J., and Birkeland, K. W.: Review of spatial variability of snowpack properties and its importance for avalanche formation, Cold Regions Science and Technology, 51, 253–272, doi:10.1016/j.coldregions.2007.04.009, 2008.

Scipión, D., Mott, R., Lehning, M., Schneebeli, M., and Berne, A.: Seasonal small-scale spatial variability in alpine snowfall and snow accumulation, Water Resources Research, 49, 1446–1457, doi:10.1002/wrcr.20135, 2013.

Skaugen, T.: Modelling the spatial variability of snow water equivalent at the catchment scale, Hydrology and Earth System Sciences, 11, 1543 – 1550, doi:10.5194/hess-11-1543-2007, 2007.

Sona, G., Pinto, L., Pagliari, D., Passoni, D., and Gini, R.: Sperimental analysis of different software packages for orientation and digital surface modelling from UAV images, Earth Science Informatics, 7, 97–107, doi:10.1007/s12145-013-0142-2, 2014.

Stretcha, C., Pylyänäinen, T., and Fua, P.: Dynamic and scalable large scale image reconstruction, in: IEEE Conference on Computer Vision and Pattern Recognition, pp. 406–413, San Francisco, USA, doi:10.1109/CVPR.2010.5540184, 2010.

Verhoeven, G.: Software Review - Taking Computer Vision Aloft - Archaeological Three-dimensional Reconstructions from Aerial Photographs with PhotoScan, Archeological Prospection, 18, 67–73, 2011.

Watts, A. C., Ambrosia, V. G., and Hinkley, E. A.: Unmanned Aircraft Systems in Remote Sensing and Scientific Research: Classification and Considerations of Use, Remote Sensing, 4, 1671–1692, doi:10.3390/rs4061671, 2012.

Winstral, A., Marks, D., and Gurney, R.: Simulating wind-affected snow accumulations at catchment to basin scales, Advances in Water Resources, 55, 64–79, doi:10.1016/j.advwatres.2012.08.011, 2013.

Worby, A. P., Markus, T., Steer, A. D., Lytle, V. I., and Massom, R. A.: Evaluation of AMSR-E snow depth product over East Antarctic sea ice using in situ measurements and aerial photography, Journal of Geophysical Research, 113, C05S94, doi:10.1029/2007JC004181, 2008.

Table 1: Comparison between manual (H_M) and U.A.S. ($H_{U.A.S.}$) snow depth measurements.

ID	H_M [m]	$H_{U.A.S.}$ [m]	$H_M - H_{U.A.S.}$ [m]
1	1.48	1.40	0.08
2	2.07	2.06	0.01
3	1.75	1.96	-0.21
4	1.88	2.05	-0.17
5	1.68	1.93	-0.25
6	1.85	2.13	-0.28
7	1.96	2.03	-0.07
8	2.11	2.17	-0.06
9	1.91	1.96	-0.05
10	1.89	1.81	0.08
11	1.45	1.49	-0.04
12	1.60	1.52	0.08
Average difference [m]			-0.073
St. dev. difference [m]			0.128

Table 2: Snow volume calculation using U.A.S. measurements and three different spatial resolutions: 5, 10, 20 cm.

Resolution [cm]	pixels [#]	$\bar{H}$ [m]	H_{max} [m]	H_{min} [m]	V [m^3]
5	81918743	2.26	4.21	-0.22	463652.3
10	20479686	2.26	4.35	-0.24	462957.8
20	5119921	2.27	4.15	-0.24	464093.0

Table 3: Comparison between the snow volume via U.A.S. $V_{U.A.S.} = 463652.3$ m^3 and the one obtained via spatialization techniques (V_T).

Technique	V_T [m^3]	$V_{U.A.S.} - V_T$ [m^3]
Arith.c mean	369146.3	94505.9
IDW	368216.9	95435.3
Thiessen	363400.5	100251.7
Kriging	368433.1	95219.2

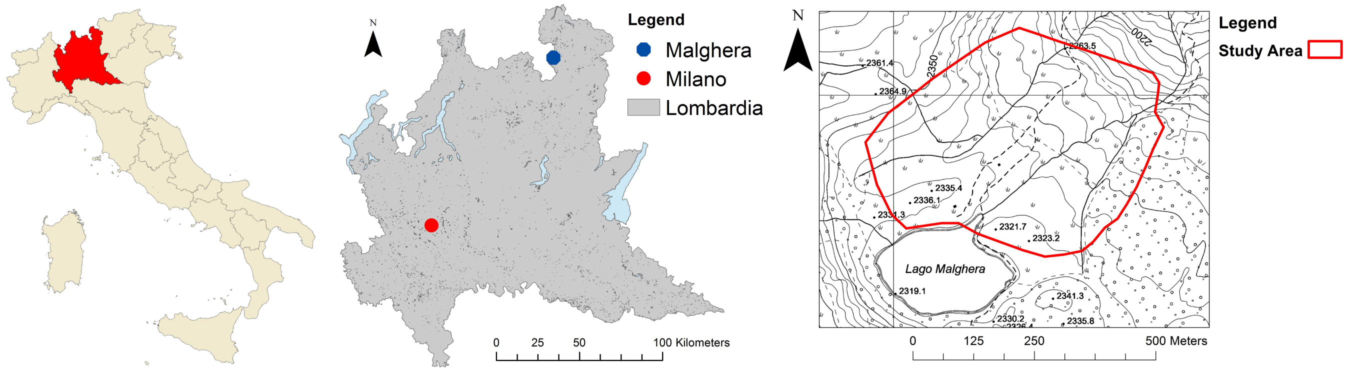

Figure 1: Location of the study area in western Val Grosina valley, Lombardia region, northern Italy. In the right panel, it is reported the topographic map of the area, with isolines every 10 m and the elevation (in m) of some points of interest.

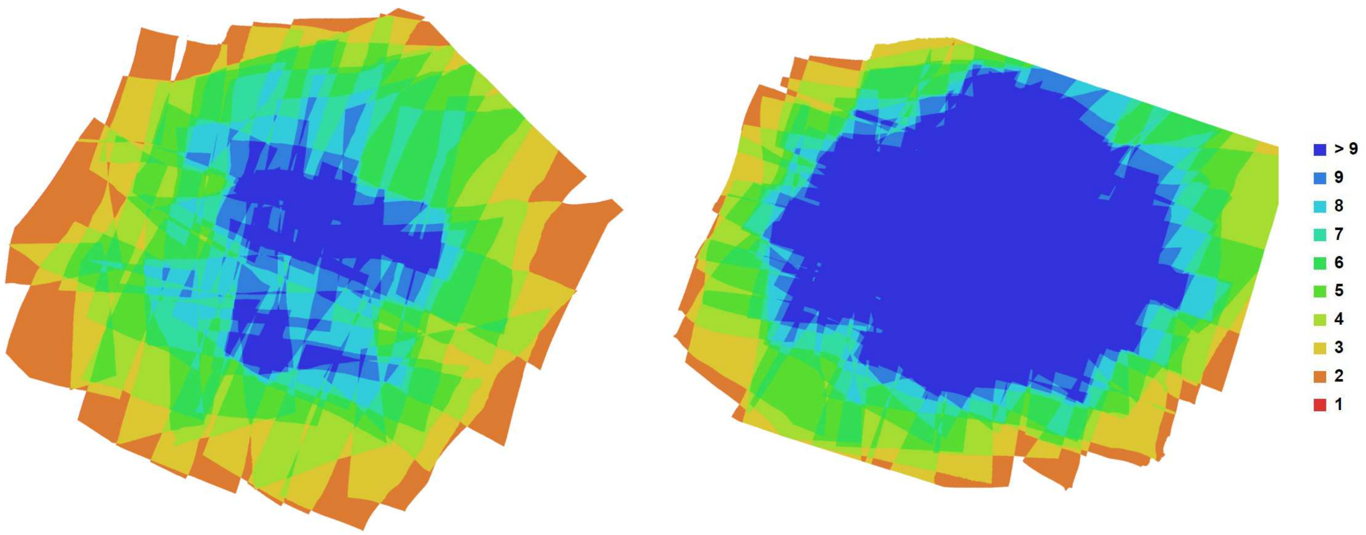

Figure 2: Camera images and their overlaps during each of the two surveys. The left panel refers to the survey made during September 2013, while the right panel regards the survey made in April 2014. The legend indicates the number of images covering each area.

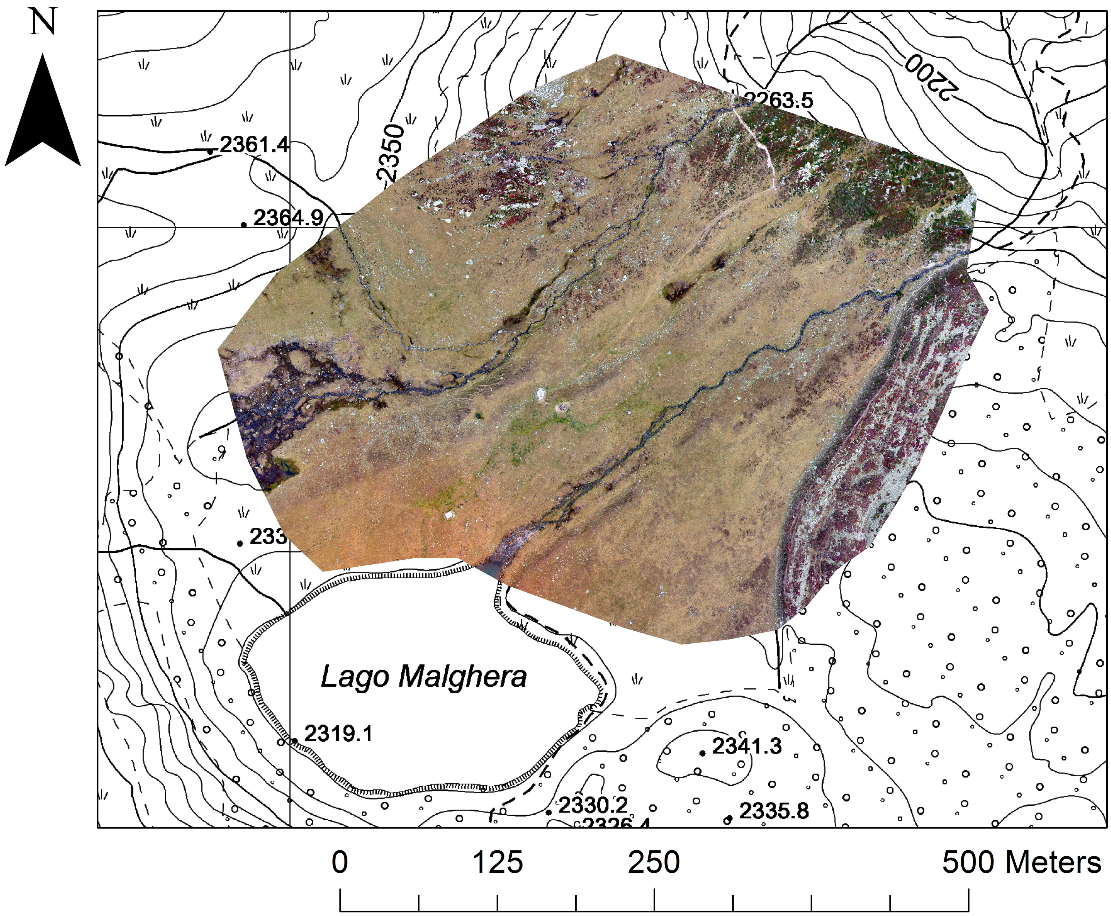

Figure 3: Ortophoto of the survey run on 26th September 2013.

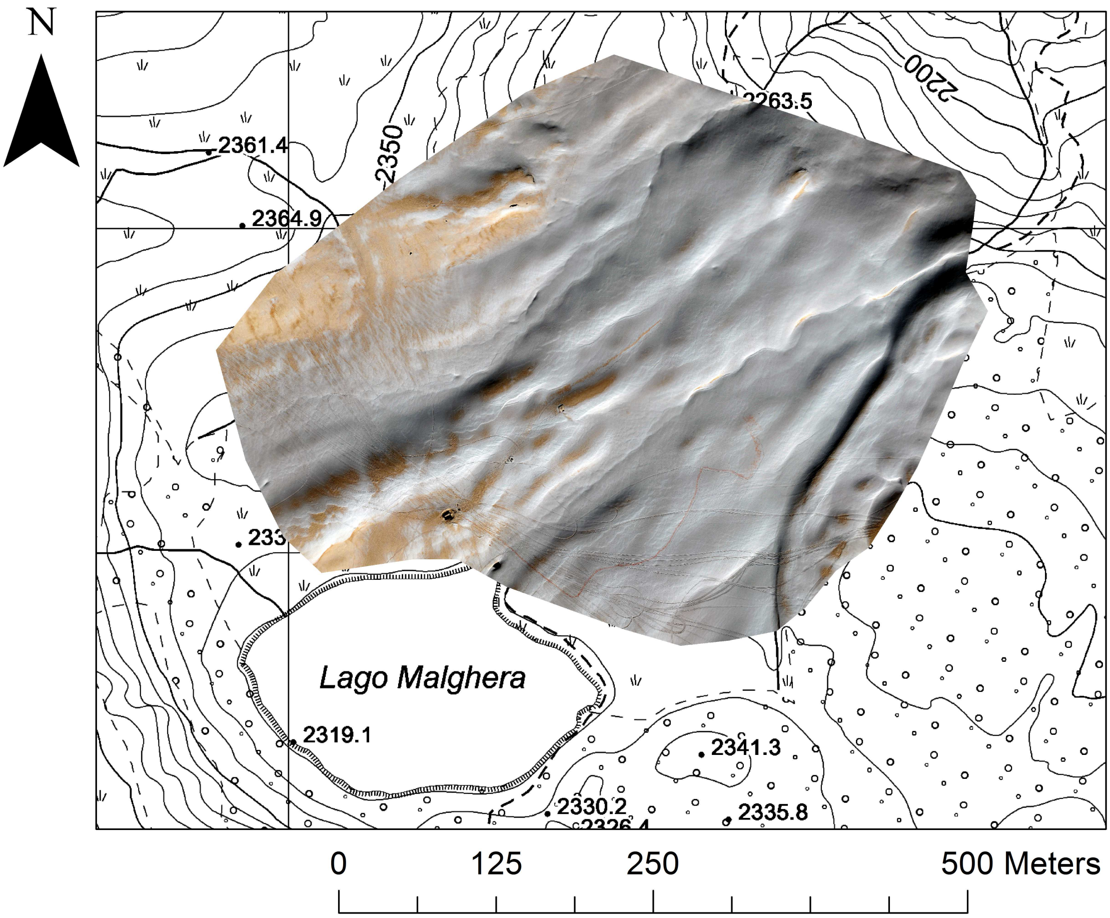

Figure 4: Ortophoto of the survey run on 11th April 2014.

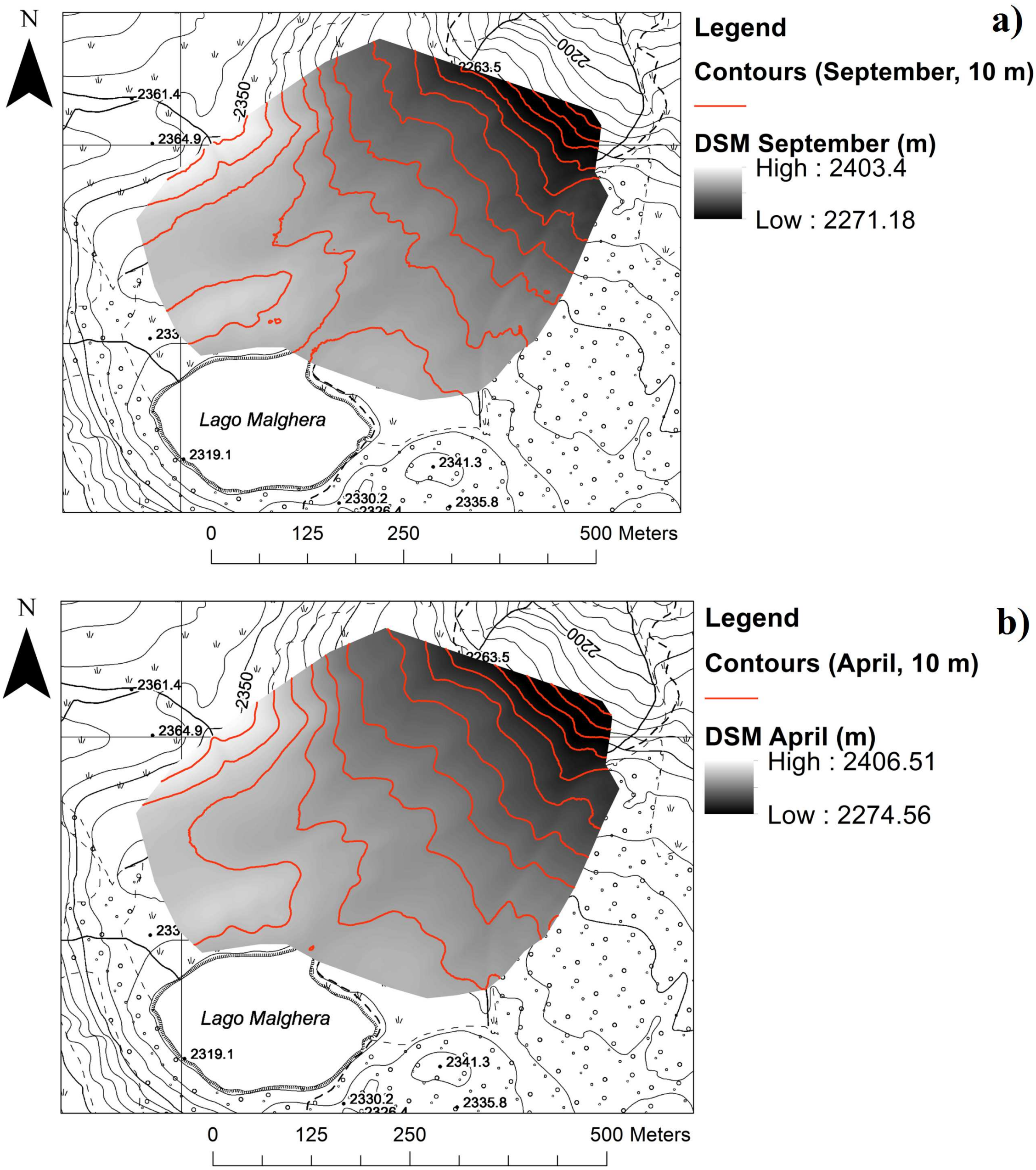

Figure 5: Digital surface model (DSM) of the two surveys. Panel a: DSM of the survey run during September 2013. Panel b: DSM of the survey run during April 2014. For both DSMs, a 5×5 cm^2 cell size has been used.

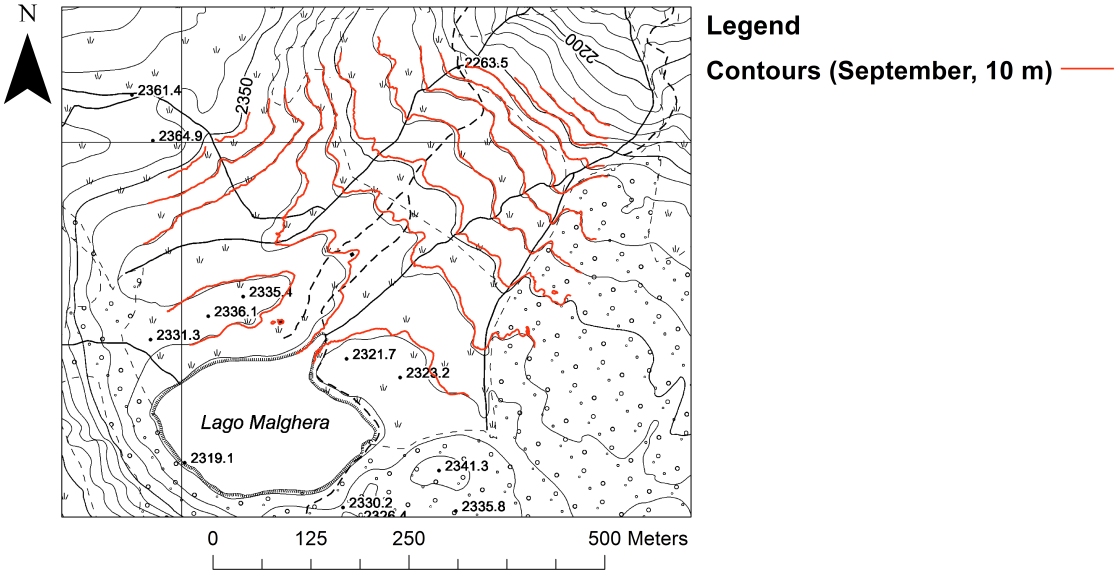

Figure 6: A comparison between U.A.S.-based contours (10 m, in red) and those reported in the topographic map of the area, see Figure 1.

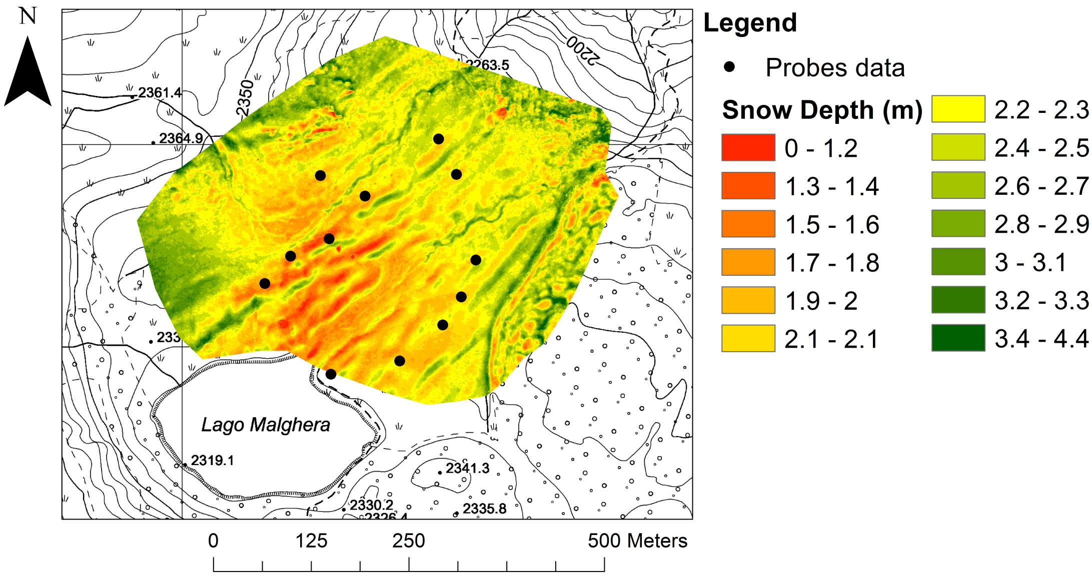

Figure 7: A map of snow depth distribution over the study area, obtained by means of difference of the elevations of the maps reported in Fig. 5. Different colors indicate different values of snow thickness (see the legend scale). Black dots indicate the location of the 12 manual measurements of snow depth.

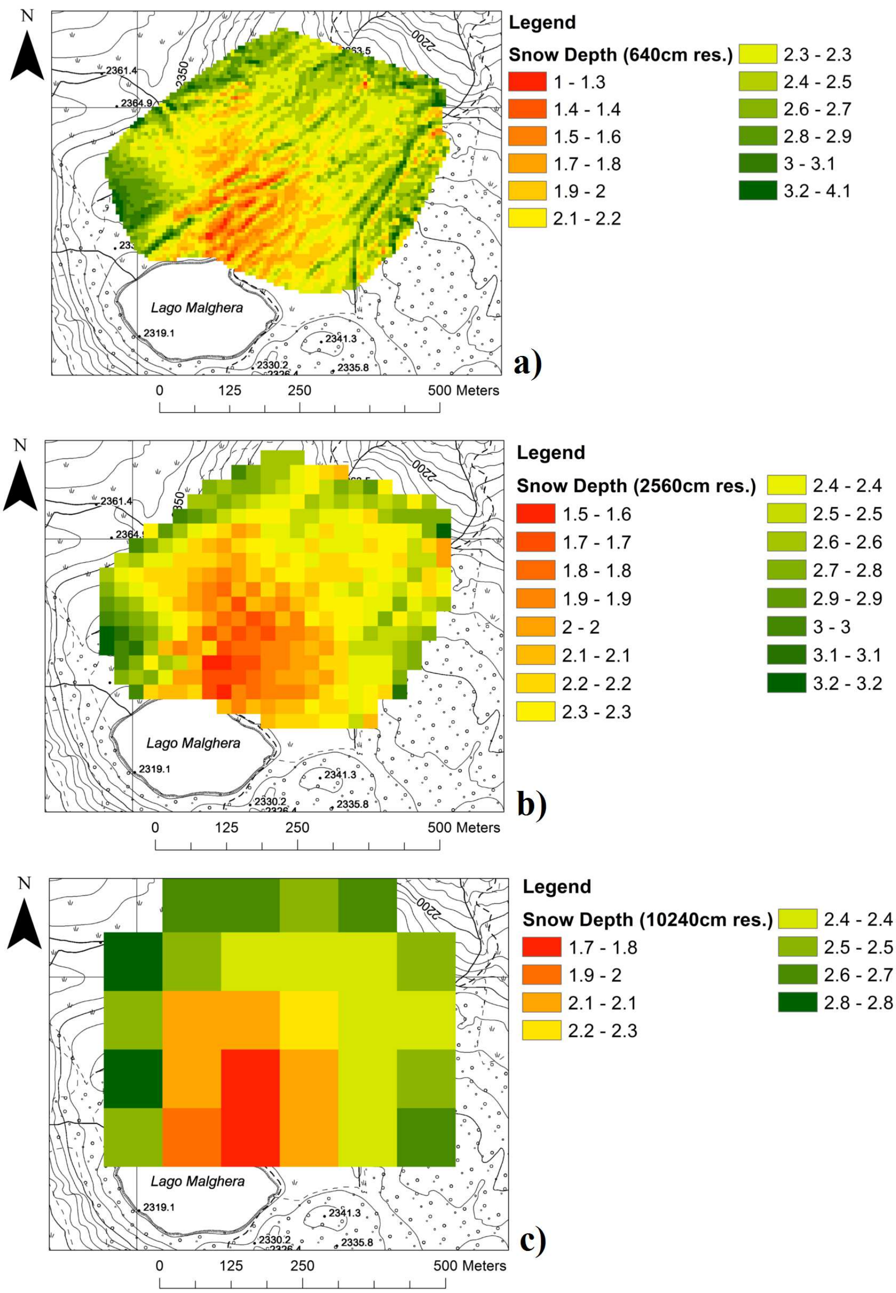

Figure 8: Rescaled maps of snow depth at different cell sizes. Panel a: 640 cm, panel b: 2560 cm, panel c: 10240 cm. See Section 4.3.2 for details.

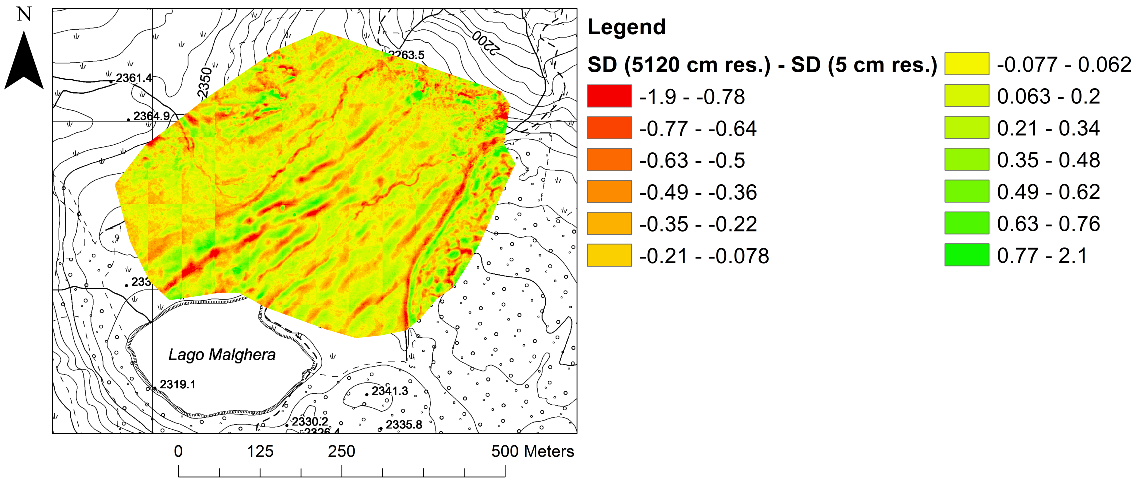

Figure 9: Differences between the rescaled map at 5120 cm resolution and the original map at 5 cm. See Section 4.3.2 for details.

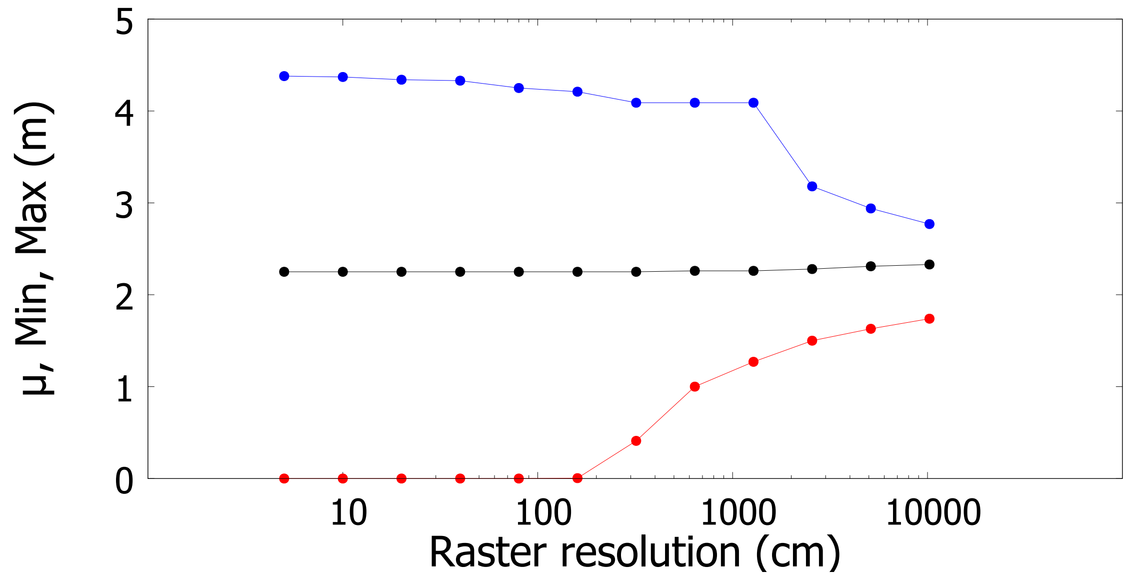

Figure 10: Mean snow depth (μ, in black), maximum and minimum values (blue and red lines, respectively) as a function of resolution.

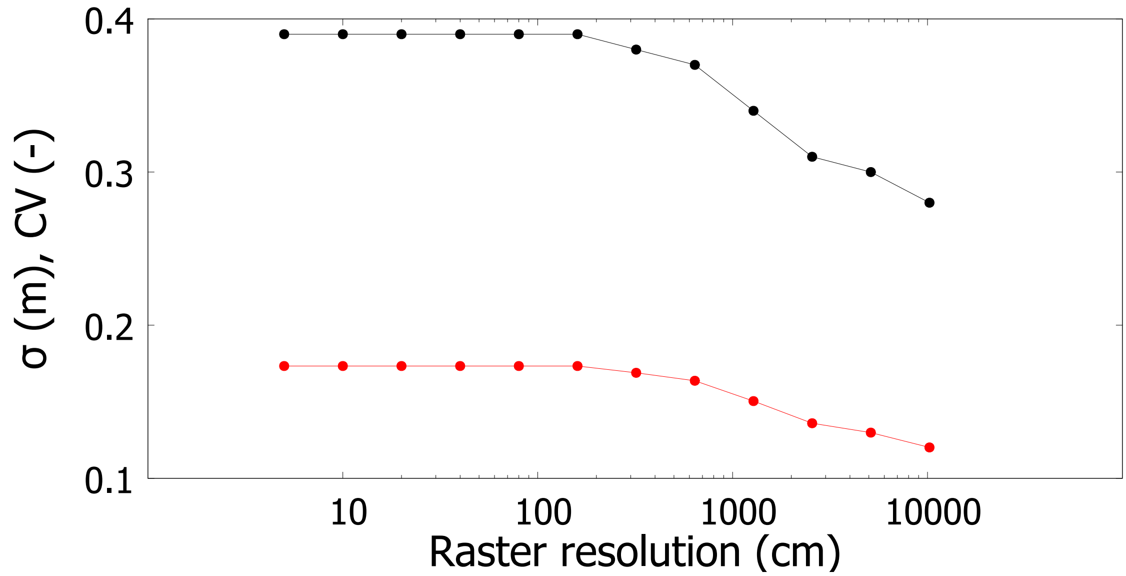

Figure 11: Standard deviation σ (black line) and CV (red line) of snow depth as a function of resolution.